Toward the Discovery of New Elements: Production of Livermorium (Z=116) with ^{50}Ti

Gates, J.M.; Orford, R.; Rudolph, D.; Appleton, C.; Barrios, B.M.; Benitez, J.Y.; Bordeau, M.; Botha, W.; Campbell, C.M.; Chadderton, J.; Chemey, A.T.; Clark, R.M.; Crawford, H.L.; Despotopulos, J.D.; Dorvaux, O.; Esker, N.E.; Fallon, P.; Folden, C.M.; Gall, B.J.P.; Garcia, F.H.; Golubev, P.; Gooding, J.A.; Grebo, M.; Gregorich, K.E.; Guerrero, M. ; Henderson, R. A.; Herzberg, R. -D.; Hrabar, Y.; King, T.T.; Kireeff Covo, M.; Kirkland, A.S.; Krücken, R.; Leistenschneider, E.; Lykiardopoulou, E.M.; McCarthy, M.; Mildon, J.A.; Müller-Gatermann, C.; Phair, L.; Pore, J.L.; Rice, E.; Rykaczewski, K.P.; Sammis, B.N.; Sarmiento, L.G.; Seweryniak, D; Sharp, D.K.; Sinjari, A.; Steinegger, P.; Stoyer, M.A.; Szornel, J.M.; Thomas, K.

Published in:
Physical Review Letters

DOI:
10.1103/PhysRevLett.133.172502

2024

LUND UNIVERSITY

PO Box 117
221 00 Lund
+46 46-222 00 00

Editors' Suggestion   Featured in Physics

Toward the Discovery of New Elements: Production of Livermorium ($Z = 116$) with ^{50}Ti

J. M. Gates,[1,*] R. Orford,[1] D. Rudolph,[2,1] C. Appleton,[1] B. M. Barrios,[3] J. Y. Benitez,[1] M. Bordeau,[4] W. Botha,[3] C. M. Campbell,[1] J. Chadderton,[5] A. T. Chemey,[6] R. M. Clark,[1] H. L. Crawford,[1] J. D. Despotopulos,[7] O. Dorvaux,[4] N. E. Esker,[3] P. Fallon,[1] C. M. Folden III,[8,9] B. J. P. Gall,[4] F. H. Garcia,[1,†] P. Golubev,[2,1] J. A. Gooding,[1,10] M. Grebo,[1,10] K. E. Gregorich,[7] M. Guerrero,[3] R. A. Henderson,[7] R.-D. Herzberg,[5] Y. Hrabar,[2] T. T. King,[11] M. Kireeff Covo,[1] A. S. Kirkland,[8,9] R. Krücken,[1] E. Leistenschneider,[1] E. M. Lykiardopoulou,[1] M. McCarthy,[1,10] J. A. Mildon,[8,9] C. Müller-Gatermann,[12] L. Phair,[1] J. L. Pore,[1] E. Rice,[1,10] K. P. Rykaczewski,[11] B. N. Sammis,[7] L. G. Sarmiento,[2] D. Seweryniak,[12] D. K. Sharp,[13] A. Sinjari,[1,10] P. Steinegger,[14,15] M. A. Stoyer,[7,1] J. M. Szornel,[1] K. Thomas,[7] D. S. Todd,[1] P. Vo,[3] V. Watson,[1] and P. T. Wooddy[7]

[1]*Nuclear Science Division, Lawrence Berkeley National Laboratory, Berkeley, California 94720, USA*
[2]*Department of Physics, Lund University, 22100 Lund, Sweden*
[3]*San Jose State University, San Jose, California 95192, USA*
[4]*Université de Strasbourg, CNRS, IPHC UMR 7178, 67037 Strasbourg, France*
[5]*University of Liverpool, Liverpool, United Kingdom*
[6]*Oregon State University, Corvallis, Oregon 97331, USA*
[7]*Lawrence Livermore National Laboratory, Livermore, California 94550, USA*
[8]*Cyclotron Institute, Texas A&M University, College Station, Texas 77843, USA*
[9]*Department of Chemistry, Texas A&M University, College Station, Texas 77843, USA*
[10]*University of California, Berkeley, California 94720, USA*
[11]*Oak Ridge National Laboratory, Oak Ridge, Tennessee 37831, USA*
[12]*Argonne National Laboratory, Lemont, Illinois 60439, USA*
[13]*University of Manchester, Manchester, United Kingdom*
[14]*Department of Chemistry and Applied Biosciences, ETH Zürich, Zurich, Switzerland*
[15]*Nuclear Energy and Safety Division, Paul Scherrer Institute, Villigen PSI, Switzerland*

(Received 3 July 2024; accepted 3 September 2024; published 21 October 2024)

The ^{244}Pu(^{50}Ti, xn)$^{294-x}$Lv reaction was investigated at Lawrence Berkeley National Laboratory's 88-Inch Cyclotron. The experiment was aimed at the production of a superheavy element with $Z \geq 114$ by irradiating an actinide target with a beam heavier than ^{48}Ca. Produced Lv ions were separated from the unwanted beam and nuclear reaction products using the Berkeley Gas-filled Separator and implanted into a newly commissioned focal-plane detector system. Two decay chains were observed and assigned to the decay of ^{290}Lv. The production cross section was measured to be $\sigma_{\text{prod}} = 0.44(^{+0.58}_{-0.28})$ pb at a center-of-target center-of-mass energy of 220(3) MeV. This represents the first published measurement of the production of a superheavy element near the "island of stability," with a beam of ^{50}Ti and is an essential precursor in the pursuit of searching for new elements beyond $Z = 118$.

DOI: 10.1103/PhysRevLett.133.172502

The production of superheavy elements (SHE), and the investigation of their properties, stands as an important frontier in modern nuclear physics [1]. The existence of SHE was first theorized in the 1950s as the result of stabilization of very heavy ($A \approx 300$), neutron-rich ($N \approx 184$) nuclei due to the presence of closed nuclear shells [2–5]. Today, the concept of an "island of stability" remains an intriguing topic [6], with its exact position and extent on the Segré chart continuing to be a subject of active pursuit both in theoretical and experimental nuclear physics [7–14].

Over the decades, SHE from $Z = 104$–118 were discovered using different types of nuclear reactions: first by impinging light ions on actinide targets in so-called "hot-fusion" reactions [15], and then by using transition metal beams (e.g., ^{50}Ti-^{70}Zn) on targets of Pb or Bi, in so-called "cold-fusion" reactions. The production of SHE from both of these reaction mechanisms showed similar properties—quickly decreasing cross sections with increasing Z of the compound nucleus. The heaviest element produced with one of these reactions was Nh ($Z = 113$), using the ^{209}Bi(^{70}Zn, n) reaction. At a cross section of just $\sigma_{\text{prod}} = 22(^{+20}_{-13})$ fb [16,17], only three ^{278}Nh nuclei were registered

*Contact author: jmgates@lbl.gov
†Present address: Department of Chemistry, Simon Fraser University, Burnaby, British Columbia V5A 1S6, Canada.

in over 500 days of beam time, seeming to mark the end of new SHE production. Fortunately, a major breakthrough was under way with the production of SHE by irradiating actinide targets from ^{238}U to ^{249}Cf with beams of ^{48}Ca [18]. Between 2000 and 2016, five new elements were added to the periodic table [19] and over 50 isotopes with $Z = 104$–118 were discovered [20]. Since many of these are located near the island of stability, these discoveries have provided crucial insights into the chemistry and physics of SHE [21]. One of the key focuses of the field is now on the production of new SHE.

Presently, Og ($Z = 118$) marks the limit for the production of SHE using ^{48}Ca beams. To attempt production of elements with $Z = 119$ or 120 using ^{48}Ca, targets of Es or Fm would be required. Neither of these elements can be produced in sufficient quantities to produce a suitable target [22]. A new reaction approach is required. Numerous theoretical studies have predicted the production rate of new elements using actinide targets and beams heavier than ^{48}Ca [23–42]. Most models reproduce the known excitation functions for the production of SHE with ^{48}Ca beams on actinide targets reasonably well. They also largely agree that reactions with ^{50}Ti have the highest cross sections for the production of elements with $Z = 119$ and 120. But the similarities end there. As shown in Fig. 1, the predicted cross sections for the ^{50}Ti + ^{249}Cf reaction span more than 3 orders of magnitude. Further, proposed beam energies for maximum production differ by tens of MeV. Notably, these predictions are highly sensitive to the mass models used in the calculations [23,24], and there are no mass measurements in the region with which to anchor the mass models. The disagreements within theoretical cross sections are currently hindering experimental efforts: The expected low cross sections imply that only one event every

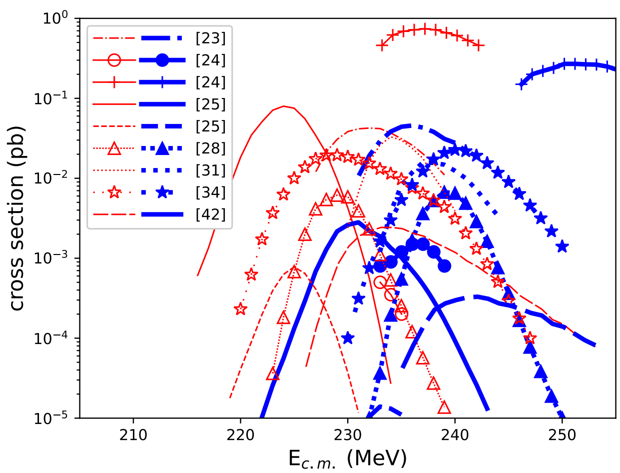

FIG. 1. Theoretical predictions of cross sections for the production of element $Z = 120$ from the $3n$ (thin red lines) and $4n$ (thick blue lines) exit channels of the ^{50}Ti + ^{249}Cf reaction [23–25,28,31,34,42].

few weeks or months could be detected under ideal experimental settings. Further, choosing the correct excitation energy of the compound nucleus that corresponds to the maximum cross section is absolutely critical. If experimental settings are off by only a few MeV, the production rate may decrease dramatically.

Several experimental campaigns have attempted to make new elements with $Z = 119$, 120, and 122 using the reactions ^{64}Ni + ^{238}U [43], ^{58}Fe + ^{244}Pu [44], ^{50}Ti + ^{249}Bk [45], ^{50}Ti + ^{249}Cf [45], and ^{70}Zn + ^{238}U [46]. All have been unsuccessful to date, reaching one-event cross-section limits of 0.09, 0.4, 0.065, 0.2, and 7.2 pb, respectively. Notably, these published upper-limit values are not able to sufficiently constrain theoretical predictions. Recently, a press release claimed the production of the new isotope ^{288}Lv in the reaction ^{54}Cr + ^{238}U [47]. However, no publication is presently available regarding the observed event(s), the measured cross section, or the utilized experimental setup. There is a report on the possible production of element 120 using the reaction ^{54}Cr + ^{248}Cm [48]. Other members of that collaboration attribute the same decay chain to a sequence of random events [49].

It is important to test these new production mechanisms for elements where cross sections are predicted to be more accessible. We investigated the production of Lv ($Z = 116$) using the ^{50}Ti + ^{244}Pu reaction. Several groups have published theoretical excitation functions or cross-section predictions for both this reaction and reactions with ^{50}Ti beams to make elements with $Z \geq 119$ [23,30,36,50]. The authors of Ref. [23] predict that ^{290}Lv can be produced at a cross section of $\approx$0.2 pb at an excitation energy of $\approx$45 MeV, whereas the authors of Ref. [36] report a maximum cross section of $\approx$ 0.1 pb at an excitation energy of $\approx$39 MeV. Reference [30] contains two predictions created with different mass models, both of which give a cross section of $\approx$0.05 pb at an excitation energy of $\approx$40 MeV. A further calculation indicates that the cross section is between 0.12 and 0.86 pb [50]. Measuring the cross section of this reaction would be an important benchmark for constraining theoretical predictions.

Here we report on the first results from the ^{244}Pu(^{50}Ti, xn)$^{294-x}$Lv experiment using the Berkeley Gas-filled Separator (BGS) [51] at Lawrence Berkeley National Laboratory's (LBNL) 88-Inch Cyclotron facility.

Isotopically enriched ^{50}Ti ($\geq 90\%$) was acquired as ^{50}TiO$_2$ and reduced to its metallic form at Argonne National Laboratory. The metallic ^{50}Ti was then used to produce a ^{50}Ti^{12+} beam from the Versatile ECR for NUclear Science (VENUS) ion source [52,53] using a newly developed induction oven [54]. The average beam intensity out of VENUS was $\approx$ 100 electrical$*\mu$A. This beam was accelerated to energies of 282(3) MeV using the LBNL 88-Inch Cyclotron. The beam energy was measured at the start of each campaign by nondestructively measuring the time of flight of individual beam pulses between two fast-current transformers separated by 3.563(5) m along a neighboring beam line [55]. The average ^{50}Ti beam intensity was $\approx 6 \times 10^{12}$ ions per second at the exit of the cyclotron. After acceleration, the beam passed through a differential pumping section that isolated the vacuum of the cyclotron from the 0.45-Torr He fill gas within the BGS. Collimators within the differential pumping section may reduce the beam intensity on target as compared to that at the exit of the cyclotron.

The beam then impinged on the target composed of four arc-shaped segments forming a rotating target wheel with a diameter of 12.2 cm. A fast-acting beam chopper can interrupt the beam in case of system failures, protecting the target [56]. Each target segment consisted of a 2.1(1)-μm-think ^{nat}Ti backing foil onto which ^{244}Pu had been electrodeposited. The electrodeposition was performed at Lawrence Livermore National Laboratory. The beam first passed through the Ti foil before entering the ^{244}Pu layer. Prior to irradiation, the target foils were measured to have an average target thicknesses of 0.435(40) mg/cm^2 ^{244}Pu (as ^{244}PuO$_2$) through γ-ray analysis of the decay of the short-lived ^{240m}Np, which is part of the decay path originating from ^{244}Pu. Note that some target material is sputtered during irradiation and that these targets were also previously irradiated for ten days during a ^{244}Pu(^{48}Ca, xn) experiment. They may thus be thinner than when initially produced.

To allow for cross-section calculations, two silicon pin-diode detectors were positioned at angles of $\pm 27.2(1)°$ directly from the beam direction. These detectors monitor the integral of beam intensity times target thickness through the detection of Rutherford-scattered beam particles.

Energy losses of the beam in the targets were assessed with SRIM2013 [57]. The beam was estimated to have lost 15(1) MeV passing through the backing foil and an additional 3 to 5 MeV passing through the ^{244}Pu target layer, depending on the target thickness of the segment. This yields an average center-of-target center-of-mass frame energy of 220(3) MeV, which corresponds to an average compound-nucleus excitation energy of 41(2) MeV according to the Thomas-Fermi mass tables [58].

The targets were irradiated for a total of 22.1 days. During these measurements, the recoiling evaporation residues (EVRs) were separated from the beam and unwanted nuclear reaction products in the BGS [51] based on their differing magnetic rigidities ($B\rho$) in 0.45-Torr He. The BGS was initially set to bend reaction products with $B\rho = 2.19$ T m to its focal plane. This was increased to $B\rho = 2.24$ T m for the last $\approx$3.1 days. The efficiency for transporting Lv EVRs through the BGS was estimated to be 70(7)% [51]. For the efficiency simulations, it was assumed that the BGS $B\rho$ was tuned such that Lv EVRs were centered in the focal-plane detector.

At the BGS focal plane, the EVRs were implanted into the SuperHeavy RECoil (SHREC) detector provided by Lund University [59]. SHREC and its readout system were previously commissioned at the BGS focal plane using ^{254}No EVRs produced in the ^{208}Pb(^{48}Ca, 2n) reaction [60] and $^{288-289}$Fl EVRs produced in the ^{244}Pu(^{48}Ca, 3–4n) reaction. In brief, SHREC has an implantation detector that is situated perpendicular to the path of the beam. This detector is comprised of three side-by-side double-sided silicon-strip detectors (DSSDs). Each DSSD has an active area of 58.5×58.5 mm^2 and is subdivided into 58 strips on both the front side (junction) and the rear side (Ohmic). On the front side of the detector, the 174 strips denote position in the horizontal direction. On the back sides of the detector, the 58 strips were wire bonded across all three DSSDs, yielding 58 strips denoting vertical position. Directly downstream of the implantation detector is an identical set of three DSSDs that serve to veto signals from light, high-energy, charged particles. These particles pass through the 300-μm implantation detector, depositing only a portion of their energy in the implantation and veto detectors. They may thus mimic escape- and α-like events. Upstream of the implantation detector is a "tunnel" of eight DSSDs which can catch the remaining energy fraction of α particles that escape from the face of the implantation detector. The geometric efficiency of SHREC for detecting a full-energy α particle in the implantation detector is $\gtrsim$50%. Depending on the implantation profile, reconstructed α decays that split their energy deposition between the implantation detector and the upstream detectors increase the efficiency to 75%–80% [59,60].

Signals from all DSSDs were processed with compact charge-sensitive preamplifiers [61] and sent to ten 64-channel CAEN VX2740 digitizers (16 bit, up to 125 MS/s). Each digitizer channel self-triggered above an energy threshold of $\cong$ 200 keV. Signals were processed using the Digital Pulse Processing Pulse Height Analysis firmware controlled through the CoMPASS software from CAEN [62]. Waveforms (30 μs long), timestamps, detector strip identifiers, and uncalibrated "energies" from an online trapezoidal filter were recorded for all events [59,60]. Energy calibrations were performed for SHREC before and after each experiment using α sources consisting of ^{148}Gd, ^{239}Pu, ^{241}Am, and ^{244}Cm, and a ^{207}Bi conversion-electron source. This calibration technique was previously optimized using α-decay lines of implanted ^{254}No and ^{250}Fm [60].

The expected reaction products of this experiment were from the 3n and 4n exit channels, ^{291}Lv and ^{290}Lv, respectively. The decay properties of both isotopes and their daughters have previously been published through their production both directly and indirectly in the ^{249}Cf(^{48}Ca, 3n) [63,64], ^{245}Cm(^{48}Ca, 2–3n) [63–65], ^{244}Pu(^{48}Ca, 5n) [63], and ^{242}Pu(^{48}Ca, 3–4n) [14,66–69] reactions. A discussion of the search parameters for decay

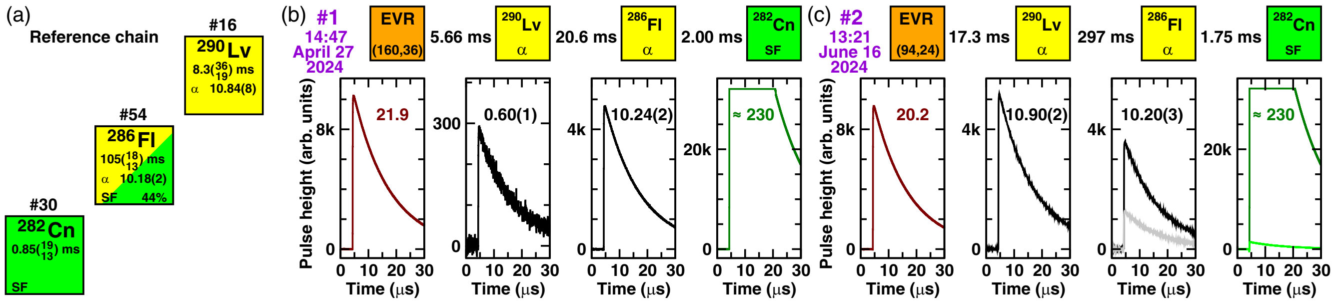

FIG. 2. (a) Reference α-decay chain of ^{290}Lv [70]. Lifetimes, α-particle energies, and branching ratios are based on published data of decay events associated with ^{290}Lv, ^{286}Fl, and ^{282}Cn [14,63–69,71]. The number of events previously observed for each isotope is signified by #N above each isotope. (b) Waveforms of preamplifier pulses of the decay chain #1 assigned to ^{290}Lv. Numbers in the panels are calibrated detected energies in MeV. Correlation times are given between recoil implantation (orange), α decays (yellow), and fission (green). The decay chain was observed in pixel (160,36). (c) Same as (b) but for decay chain #2 assigned to ^{290}Lv. The decay chain was observed in pixel (94,24). The waveforms in lighter colors in the two rightmost graphs were registered in the neighboring pixel (93,24).

chains originating from ^{291}Lv is included in Supplemental Material [70]. During the present campaigns, no decay chains were observed that fit the known decay properties of ^{291}Lv and its daughters.

Data from published decay chains of ^{290}Lv are summarized in Fig. 2(a), Fig. 3, and Ref. [70]. Potential decay chains originating from ^{290}Lv were identified using correlations that required observing the implantation of an EVR $[10 < E(\mathrm{MeV}) < 30]$ followed by the decay of at least one full-energy α [either ^{290}Lv or ^{286}Fl, $[9.75 < E(\mathrm{MeV}) < 11.25]$] followed by a spontaneous fission (SF) event ($E > 120$ MeV). All three events must occur within the same (x, y) pixel of the implantation detector, and the SF must be within one second of the EVR. The efficiency for detecting a decay chain originating from ^{290}Lv under these conditions is ≈95% based on Monte Carlo simulations of decay chains with branching ratios shown in Fig. 2(a). The number of expected decay chains arising from correlations of random background events was calculated for each pixel individually, based on the rate of EVR-, α-, and SF-like events in that pixel, then summed across the entire detector. The median rate of EVR-, α-, and SF-like events was 1.2×10^{-4}, 1.4×10^{-5}, 5.1×10^{-8} Hz/pixel, respectively. The probability for random background events to form a chain that would be detected using these search conditions is 1.7×10^{-6}.

Two decay chains were observed that met the criteria above. They are shown in Figs. 2(b) and 2(c), including baseline-corrected waveforms of all constituent events. The first decay chain consisted of a 21.9-MeV EVR-like event followed 5.66 ms later by a 0.60(1)-MeV escapelike event in the same pixel. An α-like event was observed 20.6 ms after the escape. The detected energy was $E = 10.24(2)$ MeV, which includes the α-particle energy and the energy from the recoiling daughter nucleus. Following procedures outlined in Ref. [72], the α-particle energy was calculated to be $E_\alpha = 10.16(2)$ MeV. The α energy and lifetime are consistent with the known decay properties of ^{286}Fl and were

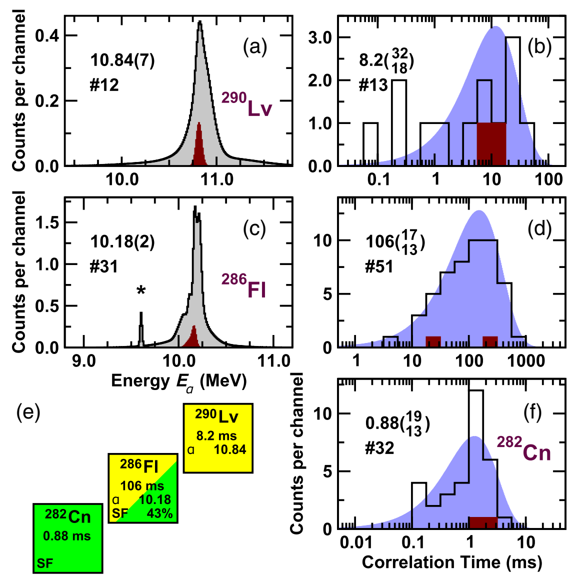

FIG. 3. Compilation of information on the decays of ^{290}Lv, ^{286}Fl, and ^{282}Cn [14,63–69,71]. Panels (a) and (c) provide experimental decay-energy spectra from events associated with the decay steps ^{290}Lv → ^{286}Fl and ^{286}Fl → ^{282}Cn, respectively. For a single entry, a Gaussian with integral one and a width compliant with its measured uncertainty was added into the spectra. The numbers in the top left of these panels are the α-decay energies, in MeV, extracted from the histogram mean in the intervals [10.0,11.7] and [9.9,10.5] MeV, respectively. The right column [(b),(d),(f)] shows the correlation times of the decays along the decay chain starting with ^{290}Lv. Experimental data points are comprised in the histograms (black lines). The shaded areas (blue) provide correlation-time distributions expected for the corresponding half-life, $T_{1/2}$ in ms, which are given in the top left corner of each panel. For all panels, the number after the hashtag # indicates the number of available data points. Entries marked in dark red correspond to the events associated with the observation of ^{290}Lv in this work. The 9.6-MeV peak marked with an * in (c) was explained in detail in [14]. Panel (e) shows the revised aggregated information of the ^{290}Lv decay chain including the events from this work (cf. Fig. 2) [70].

assigned accordingly. Based on its observed lifetime and position in the decay chain, the 0.60(1)-MeV escapelike event was assigned to an α decay of ^{290}Lv where the α particle escaped out of the front of the implantation detector and did not impact one of the upstream detectors. Thus, only a fraction of its decay energy was recorded [see, e.g., the spectra in Fig. 2(a) in Supplemental Material of Ref. [72]]. The rate of escapelike events $[0.2 < E(\mathrm{MeV}) < 6.0]$ was 7.8×10^{-3} Hz per pixel. The probability for observing a random escapelike event in the 26 ms between the EVR and the first observed full-energy α decay in the chain is 2.0×10^{-4}. The observed decay assigned to ^{286}Fl was followed just 2.00 ms later by an ≈230-MeV SF-like event. The approximate energy of the SF-like event was determined by constructing an unsaturated waveform from the unsaturated portions of the recorded waveform using benchmarked pole-zero corrections [59] and then extracting the pulse height using a trapezoidal energy filter. The lifetimes, decay modes, and decay energies of the events above are fully consistent with a decay chain consisting of a ^{290}Lv EVR implanting into SHREC, followed by the ^{290}Lv α escaping the front of SHREC, a full-energy α decay of ^{286}Fl, and terminating with the SF of ^{282}Cn [cf. Figs. 2(a) and 3].

The second decay chain [Fig. 2(c)] consisted of a 20.2-MeV EVR followed 17.3 ms later by a recoil-corrected $E_\alpha = 10.81(3)$-MeV full-energy α. A second full-energy α with $E_\alpha = 10.12(4)$ MeV was detected 297 ms later. The decay chain was terminated by an ≈230-MeV SF-like event 1.75 ms after the second α particle. Based on the energies, lifetimes, and decay modes, this series of events was assigned to a decay chain consisting of an implanted ^{290}Lv EVR followed by α decays of ^{290}Lv and ^{286}Fl, and terminating with SF of ^{282}Cn. The probability of observing two chains composed of random background events based on the rates discussed above was 1.4×10^{-12}.

The cross section for two events derived from the observed number of Rutherford-scattered particles is $\sigma_{\mathrm{prod}} = 0.44(^{+0.58}_{-0.28})$ pb at the 68% confidence level [73,74]. The error represents statistical (counting) errors only. There is also systematic error on the cross section, discussed in detail in [75], which results in an additional 12% systematic uncertainty in the measured cross sections. In cases where the reaction is run in the BGS for the first time and the $B\rho$ through the BGS is unknown, there is an additional uncertainty in detection efficiency.

The two-event cross section reported in this work is higher than theoretical predictions of Refs. [23,30,36], and all three references can be excluded at the 68% confidence level at the experimental excitation energy of 41(2) MeV. The cross section is consistent with the theoretical prediction from Ref. [50]. The observation of the two events at an excitation energy of 41(2) MeV is also consistent with the proposed optimal excitation energies in Refs. [30,36], although lower than that from [23].

The $4n$ reaction between ^{48}Ca and ^{244}Pu has been investigated previously and has been observed to have a cross section between $\sigma_{\mathrm{prod}} = 5.3(^{+3.6}_{-2.1})$ pb [65,72] and $\sigma_{\mathrm{prod}} = 9.8(^{+3.9}_{-3.1})$ pb [76]. These values are ≈10–20 times larger than the cross section reported in this work between ^{50}Ti and ^{244}Pu with the same exit channel. This indicates that the cross section for the production of element 120 with ^{50}Ti beams could be ≈25–50 fb based on the known $^{249}\mathrm{Cf}(^{48}\mathrm{Ca}, 3n)$ cross section of $\sigma_{\mathrm{prod}} = 0.5(^{+1.6}_{-0.3})$ pb [64], demonstrating that a substantial, but seemingly manageable, reduction in production cross sections has to be expected in the push toward discovering higher-Z elements with beams beyond ^{48}Ca.

In summary, at the LBNL 88-Inch Cyclotron facility, a ^{244}Pu target was irradiated with a high-intensity beam of ^{50}Ti. Two decay chains were observed and assigned to the decay of ^{290}Lv with a production cross section of $\sigma_{\mathrm{prod}} = 0.44(^{+0.58}_{-0.28})$ pb at a center-of-target excitation energy of 41(2) MeV. This is the first reported production of a SHE near the predicted island of stability with a beam other than ^{48}Ca. While the cross section observed here does reflect the expected decrease in SHE production when moving to heavier beams, the success of this measurement validates that discoveries of new SHE are indeed within experimental reach.

Acknowledgments—We gratefully acknowledge the operations staff of the 88-Inch Cyclotron for providing the intense beams of ^{50}Ti and stable operating conditions. This work was supported in part by the U.S. Department of Energy, Office of Science, Office of Nuclear Physics under Contracts No. DE-AC02-05CH11231 (LBNL), No. DE-AC02-06CH11357 (ANL), and No. DE-FG02-93ER40773 (TAMU); U.S. Department of Energy, Office of Science, Office of Basic Energy Sciences under Contracts No. DE-AC02-05CH11231 (LBNL); the Swedish Knut and Alice Wallenberg Foundation (Grant No. KAW 2015.0021), the Wenner-Gren Foundations (Grant No. SSv2020-0003), the Carl Trygger Foundation (Grant No. CTS 20:1146), and the Royal Physiographic Society in Lund; UK Science and Technology Facilities Council under Grants No. ST/V001027/1 (Liverpool), No. ST/T004797/1, and No. ST/V001116/1 (Manchester); startup package from the Oregon State University College of Engineering; Office of Nuclear Regulatory Research, Nuclear Regulatory Commission under Grant No. 31310022M0019 (SJSU); U.S. Department of Energy under Contracts No. DE-AC52-07NA27344 (LLNL) and No. DE-AC05-00OR22725 (ORNL); Swiss National Science Foundation under Grant No. 200020_196981; CNRS research funds

(IPHC). The authors are indebted (for the use of ^{244}Pu) to the U.S. Department of Energy, through the transplutonium element production facilities at Oak Ridge National Laboratory.

[1] NSAC Long Range Plan Working Group, 10.2172/2280968.
[2] G. Scharff-Goldhaber, Nuclear physics, Nucleonics **15**, 122 (1957), https://archive.org/details/sim_nucleonics_1957-09_15_9/page/122/mode/2up.
[3] W. D. Myers and W. J. Swiatecki, Nuclear masses and deformations, Nucl. Phys. **81**, 1 (1966).
[4] A. Sobiczewski, F. A. Gareev, and B. N. Kalinkin, Closed shells for $Z > 82$ and $N > 126$ in a diffuse potential well, Phys. Lett. **22**, 500 (1966).
[5] S. G. Nilsson, C. F. Tsang, A. Sobiczewski, Z. Szymański, S. Wycech, C. Gustafson, I.-L. Lamm, P. Möller, and B. Nilsson, On the nuclear structure and stability of heavy and superheavy elements, Nucl. Phys. **A131**, 1 (1969).
[6] O. R. Smits, Ch. E. Düllmann, P. Indelicato, W. Nazarewicz, and P. Schwerdtfeger, The quest for superheavy elements and the limit of the periodic table, Nat. Rev. Phys. **6**, 86 (2024).
[7] S. Ćwiok, J. Dobaczewski, P.-H. Heenen, P. Magierski, and W. Nazarewicz, Shell structure of the superheavy elements, Nucl. Phys. **A611**, 211 (1996).
[8] M. Bender, K. Rutz, P.-G. Reinhard, J. A. Maruhn, and W. Greiner, Shell structure of superheavy nuclei in self-consistent mean-field models, Phys. Rev. C **60**, 034304 (1999).
[9] A. T. Kruppa, M. Bender, W. Nazarewicz, P.-G. Reinhard, T. Vertse, and S. Ćwiok, Shell corrections of superheavy nuclei in self-consistent calculations, Phys. Rev. C **61**, 034313 (2000).
[10] S. Ćwiok, P.-H. Heenen, and W. Nazarewicz, Shape coexistence and triaxiality in the superheavy nuclei, Nature (London) **433**, 705 (2005).
[11] W. Zhang, J. Meng, S. Q. Zhang, L. S. Geng, and H. Toki, Magic numbers for superheavy nuclei in relativistic continuum Hartree–Bogoliubov theory, Nucl. Phys. **A753**, 106 (2005).
[12] A. Sobiczewski and K. Pomorski, Description of structure and properties of superheavy nuclei, Prog. Part. Nucl. Phys. **58**, 292 (2007).
[13] J. L. Egido and A. Jungclaus, Predominance of triaxial shapes in transitional super-heavy nuclei: Ground-state deformation and shape coexistence along the flerovium ($Z = 114$) chain of isotopes, Phys. Rev. Lett. **125**, 192504 (2020).
[14] A. Såmark-Roth *et al.*, Spectroscopy along flerovium decay chains: Discovery of ^{280}Ds and an excited state in ^{282}Cn, Phys. Rev. Lett. **126**, 032503 (2021).
[15] S. Hofmann, Super-heavy nuclei, J. Phys. G **42**, 114001 (2015).
[16] K. Morita *et al.*, Experiment on the synthesis of element 113 in the reaction ^{209}Bi(^{70}Zn, n)^{278}113, J. Phys. Soc. Jpn. **73**, 2593 (2004).
[17] K. Morita *et al.*, New result in the production and decay of an isotope, ^{278}113, of the 113th element, J. Phys. Soc. Jpn. **81**, 103201 (2012).
[18] Yu. Ts. Oganessian, A. Sobiczewski, and G. M. Ter-Akopian, Superheavy nuclei: From predictions to discovery, Phys. Scr. **92**, 023003 (2017).
[19] L. Öhrström and J. Reedijk, Names and symbols of the elements with atomic numbers 113, 115, 117 and 118 (IUPAC recommendations 2016), Pure Appl. Chem. **88**, 1225 (2016).
[20] Special issue on superheavy elements, edited by Ch. E. Düllmann, R.-D. Herzberg, W. Nazarewicz, and Yu. Ts. Oganessian [Nucl. Phys. **A944**, 1 (2015)], https://www.sciencedirect.com/journal/nuclear-physics-a/vol/944/suppl/C.
[21] *Nobel Symposium NS 160 – Chemistry and Physics of Heavy and Superheavy Elements*, edited by D. Rudolph (2016), ISBN 978-2-7598-9011-8, https://www.epj-conferences.org/articles/epjconf/abs/2016/26/contents/contents.html.
[22] J. B. Roberto, M. Du, J. G. Ezold, S. L. Hogle, J. Moon, K. Myhre, and K. P. Rykaczewski, Actinide targets for the synthesis of superheavy nuclei, Eur. Phys. J. A **59**, 304 (2023).
[23] V. Zagrebaev and W. Greiner, Synthesis of superheavy nuclei: A search for new production reactions, Phys. Rev. C **78**, 034610 (2008).
[24] G. G. Adamian, N. V. Antonenko, and W. Scheid, Feature of production of new superheavy nuclei in actinide-based complete-fusion reactions, Eur. Phys. J. A **41**, 235 (2009).
[25] A. K. Nasirov, G. Mandaglio, G. Giardina, A. Sobiczewski, and A. I. Muminov, Effects of the entrance channel and fission barrier in the synthesis of superheavy element $Z = 120$, Phys. Rev. C **84**, 044612 (2011).
[26] N. Wang, J. Tian, and W. Scheid, Systematics of fusion probability in "hot" fusion reactions, Phys. Rev. C **84**, 061601(R) (2011).
[27] Z.-H. Liu and J.-D. Bao, Role of the coupling between neck and radial degrees of freedom in evolution from dinucleus to mononucleus, Phys. Rev. C **83**, 044613 (2011).
[28] K. Siwek-Wilczyńska, T. Cap, M. Kowal, A. Sobiczewski, and J. Wilczyński, Predictions of the fusion-by-diffusion model for the synthesis cross sections of $Z = 114$–120 elements based on macroscopic-microscopic fission barriers, Phys. Rev. C **86**, 014611 (2012).
[29] N. Wang, E.-G. Zhao, W. Scheid, and S.-G. Zhou, Theoretical study of the synthesis of superheavy nuclei with $Z = 119$ and 120 in heavy-ion reactions with trans-uranium targets, Phys. Rev. C **85**, 041601(R) (2012).
[30] A. N. Kuzmina, G. G. Adamian, N. V. Antonenko, and W. Scheid, Influence of proton shell closure on production and identification of new superheavy nuclei, Phys. Rev. C **85**, 014319 (2012).
[31] Z.-H. Liu and J.-D. Bao, Possibility to produce element 120 in the ^{54}Cr + ^{248}Cm hot fusion reaction, Phys. Rev. C **87**, 034616 (2013).
[32] J. Jiang, Q. Chai, B. Wang, W. Zhao, M. Liu, and H. Wang, Investigation of production cross sections for superheavy nuclei with $Z = 116$–121 in dinuclear system concept, Nucl. Phys. Rev. **30**, 4 (2013).
[33] J. Zhang, C. Wang, and Z. Ren, Calculation of evaporation residue cross sections for the synthesis of superheavy nuclei in hot fusion reactions, Nucl. Phys. **A909**, 36 (2013).
[34] L. Zhu, W.-J. Xie, and F.-S. Zhang, Production cross sections of superheavy elements $Z = 119$ and 120 in hot fusion reactions, Phys. Rev. C **89**, 024615 (2014).

[35] V. I. Zagrebaev and W. Greiner, Cross sections for the production of superheavy nuclei, Nucl. Phys. **A944**, 257 (2015).

[36] G. G. Adamian, N. V. Antonenko, H. Lenske, and L. A. Malov, Predictions of identification and production of new superheavy nuclei with $Z = 119$ and 120, Phys. Rev. C **101**, 034301 (2020).

[37] F. Niu, P. Chen, and Z. Feng, Systematics on production of superheavy nuclei $Z = 119$–122 in fusion-evaporation reactions, Nucl. Sci. Tech. **32**, 103 (2021).

[38] J.-X. Li and H.-F. Zhang, Predictions for the synthesis of the $Z = 119$ superheavy element, Phys. Rev. C **105**, 054606 (2022).

[39] J.-X. Li and H.-F. Zhang, Predictions for the synthesis of the $Z = 120$ superheavy element, Phys. Rev. C **106**, 034613 (2022).

[40] S. H. Zhu and X. J. Bao, Possibility to synthesize $Z = 120$ superheavy nuclei with $Z > 20$ projectiles, Phys. Rev. C **108**, 014604 (2023).

[41] J.-J. Li, N. Tang, Y.-H. Zhang, M.-H. Zhang, C. Wang, X.-R. Zhang, L. Zhu, and F.-S. Zhang, Progress on production cross-sections of unknown nuclei in fusion evaporation reactions and multinucleon transfer reactions, Int. J. Mod. Phys. E **32**, 2330002 (2023).

[42] M.-H. Zhang, Y.-H. Zhang, Y. Zou, C. Wang, L. Zhu, and F.-S. Zhang, Predictions of synthesizing elements with $Z = 119$ and 120 in fusion reactions, Phys. Rev. C **109**, 014622 (2024).

[43] S. Hofmann *et al.*, Probing shell effects at $Z = 120$ and $N = 184$, GSI Scientific Report, 2008, https://repository.gsi.de/record/53523/files/GSI-Report-2009-1.pdf.

[44] Yu. Ts. Oganessian *et al.*, Attempt to produce element 120 in the ^{244}Pu + ^{58}Fe reaction, Phys. Rev. C **79**, 024603 (2009).

[45] J. Khuyagbaatar *et al.*, Search for elements 119 and 120, Phys. Rev. C **102**, 064602 (2020).

[46] S. Hofmann *et al.*, New results on elements 111 and 112, Eur. Phys. J. A **14**, 147 (2002).

[47] Press release from JINR, https://www.jinr.ru/posts/v-lyar-oiyai-vpervye-v-mire-sintezirovan-livermorij-288/.

[48] S. Hofmann *et al.*, Review of even element super-heavy nuclei and search for element 120, Eur. Phys. J. A **52**, 180 (2016).

[49] F. P. Heßberger and D. Ackermann, Some critical remarks on a sequence of events interpreted to possibly originate from a decay chain of an element 120 isotope, Eur. Phys. J. A **53**, 123 (2017).

[50] T. Cap (private communication).

[51] K. E. Gregorich, Simulation of recoil trajectories in gas-filled magnetic separators., Nucl. Instrum. Methods Phys. Res., Sect. A **711**, 47 (2013).

[52] D. Leitner, S. R. Abbott, R. D. Dwinell, M. Leitner, C. Taylor, and C. M. Lyneis, Commissioning of the superconducting ECR ion source VENUS, in *Proceedings of the 2003 Particle Accelerator Conference, 2003*, 10.1109/PAC.2003.1288847 (2003), p. 86.

[53] D. Leitner, C. M. Lyneis, S. R. Abbott, D. Collins, R. D. Dwinell, M. L. Galloway, M. Leitner, and D. S. Todd, Next generation ECR ion sources: First results of the superconducting 28 GHz ECRIS—VENUS, Nucl. Instrum. Methods Phys. Res., Sect. B **235**, 486 (2005).

[54] D. S. Todd, A novel inductive oven design to produce high-current, moderate mass ion beams for superheavy element searches, Nucl. Instrum. Method. Phys. Res. A (to be published).

[55] M. Kireeff Covo, Nondestructive synchronous beam current monitor, Rev. Sci. Instrum. **85**, 125106 (2014).

[56] M. Kireeff Covo, P. Bloemhard, J. Benitez, M. Johnson, D. Todd, J. Cruz Duran, B. Ninemire, and L. Phair, Single radio frequency bucket injection in the 88-Inch Cyclotron using a pulsed high voltage chopper, Rev. Sci. Instrum. **95**, 015112 (2024).

[57] J. F. Ziegler, M. Ziegler, and J. Biersack, SRIM—the stopping and range of ions in matter (2010), Nucl. Instrum. Methods Phys. Res., Sect. B **268**, 1818 (2010).

[58] W. D. Myers and W. J. Swiatecki, Nuclear properties according to the Thomas-Fermi model, Nucl. Phys. **A601**, 141 (1996).

[59] P. Golubev *et al.*, Source characterization of a detector for heavy and superheavy nuclei, Nucl. Instrum. Method. Phys. Res. A (to be published).

[60] R. Orford *et al.*, Commissioning of the SHREC detector with ^{254}No (to be published).

[61] P. Golubev *et al.*, The Lund–York–Cologne Calorimeter (LYCCA): Concept, design and prototype developments for a fair-nustar detector system to discriminate relativistic heavy-ion reaction products, Nucl. Instrum. Methods Phys. Res., Sect. A **723**, 55 (2013).

[62] See CAEN CoMPASS documentation at https://www.caen.it/products/compass/.

[63] Yu. Ts. Oganessian *et al.*, Heavy element research at Dubna, Nucl. Phys. **A734**, 109 (2004).

[64] Yu. Ts. Oganessian *et al.*, Synthesis of the isotopes of elements 118 and 116 in the ^{249}Cf and ^{245}Cm + ^{48}Ca fusion reactions, Phys. Rev. C **74**, 044602 (2006).

[65] Yu. Ts. Oganessian *et al.*, Measurements of cross sections for the fusion-evaporation reactions ^{244}Pu(^{48}Ca, xn)$^{292-x}$114 and ^{245}Cm(^{48}Ca, xn)$^{293-x}$116, Phys. Rev. C **69**, 054607 (2004).

[66] Yu. Ts. Oganessian *et al.*, Measurements of cross sections and decay properties of the isotopes of elements 112, 114, and 116 produced in the fusion reactions ^{233,238}U, ^{242}Pu, and ^{248}Cm + ^{48}Ca, Phys. Rev. C **70**, 064609 (2004).

[67] L. Stavsetra, K. E. Gregorich, J. Dvorak, P. A. Ellison, I. Dragojević, M. A. Garcia, and H. Nitsche, Independent verification of element 114 production in the ^{48}Ca + ^{242}Pu reaction, Phys. Rev. Lett. **103**, 132502 (2009).

[68] P. A. Ellison *et al.*, New superheavy element isotopes: ^{242}Pu(^{48}Ca, 5n)^{285}114, Phys. Rev. Lett. **105**, 182701 (2010).

[69] Yu. Ts. Oganessian *et al.*, Investigation of ^{48}Ca-induced reactions with ^{242}Pu and ^{238}U targets at the JINR superheavy element factory, Phys. Rev. C **106**, 024612 (2022).

[70] See Supplemental Material at http://link.aps.org/supplemental/10.1103/PhysRevLett.133.172502 for cross-section predictions to produce element $Z = 116$, Lv, as well as an aggregated analysis of existing data of the ^{290}Lv decay chain.

[71] Yu. Ts. Oganessian *et al.*, Production and decay of the heaviest nuclei ^{293,294}117 and ^{294}118, Phys. Rev. Lett. **109**, 162501 (2012).

[72] A. Såmark-Roth *et al.*, Spectroscopy along flerovium decay chains: III. Details on experiment, analysis, ^{282}Cn, and spontaneous fission branches, Phys. Rev. C **107**, 024301 (2023).

[73] K.-H. Schmidt, C.-C. Sahm, K. Pielenz, and H. G. Clerc, Some remarks on the error analysis in the case of poor statistics, Z. Phys. A **316**, 19 (1984).

[74] K.-H. Schmidt, A new test for random events of an exponential distribution, Eur. Phys. J. A **8**, 141 (2000).

[75] K. E. Gregorich *et al.*, Attempt to confirm superheavy element production in the $^{48}Ca + ^{238}U$ reaction, Phys. Rev. C **72**, 014605 (2005).

[76] J. M. Gates *et al.*, First superheavy element experiments at the GSI recoil separator TASCA: The production and decay of element 114 in the $^{244}Pu(^{48}Ca, 3–4n)$ reaction, Phys. Rev. C **83**, 054618 (2011).